

Article

Study on Sand-Accumulation Changes of Highway and Formation Mechanism of Sand Damage in Drifting Dunes Areas

Feng Han ^{1,*} , Chengxiang Wang ¹ , Zhibo Liu ¹ , Liangying Li ¹  and Wenhua Yin ^{1,2} ¹ School of Civil Engineering, Lanzhou Jiaotong University, Lanzhou 730070, China² Ningxia Highway Survey and Design Institute Co., Ltd., Yinchuan 750001, China

* Correspondence: hanfeng740412@mail.lzjtu.cn

Abstract: After the construction of desert highway, the physiognomy changes caused by surface wind erosion and accumulation not only seriously threaten the stability of road structure, but also have a tremendous impact on the safety of the highway operation and the maintenance work on the highway. The purpose of this paper is to explore the change of sand sedimentation and the law of sand transport along the highway in the moving dune areas, and to clarify the change of sand flow and the formation mechanism of sand damage in the moving dune areas. Taking the test section of Wuhai-Maqin Expressway in the hinterland of Tengger Desert as the research object, the on-site observation of sand accumulation and the recording of wind information by small weather stations were adopted, supplemented by CFD numerical simulation method, in order to provide reference for the construction of sand control system in moving dune areas. The study results show that: (1) Dunes not only obstruct wind-drift sand but are also the sediment source condition for forming road sand. The windward dunes near the road are affected by wind and the deposition of sand will quickly bury the road in the strong wind season. (2) Compared with highways with flat terrain, the existence of dunes affects the flow field structure and the distribution of sand sedimentation on the highway, in which, under the influence of the gathering effect, the flow velocity reaches the maximum at the top of the dune and a large low-speed recirculation zone is formed on the lee side of the dune, easily causing sand accumulation. (3) Sediment accumulates at the windward side of the embankment or dune where sandy air current is easy to saturate. However, with the increase of wind speed, in addition to the grit carried by the sandy air current itself, new sand rolled up on the windward side of the dunes also form deposits on the road surface and the amount of sand-accumulation on highway surface and leeward side tends to increase. As a result, for the highway in drifting sand dunes areas, sediment prevention and control measures should be taken actively. It is necessary to remove sediment from the road in time and reduce the moving speed of sand dunes and the deposition range of wind-sand flow, ultimately for the purpose of reducing the damage wind-sand activity causes to the highway in desert.

Keywords: highway in desert; movement of sediment; sand-accumulation principle; numerical simulation; flow field structure



Citation: Han, F.; Wang, C.; Liu, Z.; Li, L.; Yin, W. Study on Sand-Accumulation Changes of Highway and Formation Mechanism of Sand Damage in Drifting Dunes Areas. *Appl. Sci.* **2022**, *12*, 10184. <https://doi.org/10.3390/app121910184>

Academic Editor: Itzhak Katra

Received: 14 September 2022

Accepted: 8 October 2022

Published: 10 October 2022

Publisher's Note: MDPI stays neutral with regard to jurisdictional claims in published maps and institutional affiliations.



Copyright: © 2022 by the authors. Licensee MDPI, Basel, Switzerland. This article is an open access article distributed under the terms and conditions of the Creative Commons Attribution (CC BY) license (<https://creativecommons.org/licenses/by/4.0/>).

1. Introduction

Because of the influence of natural environment, the construction of desert highway inevitably faces the problem of wind-sand disaster, so that clarifying the wind-sand environment and the formation mechanism of sand damage along the highway is the premise of the construction and safe operation of the highway [1,2]. Wind-sand activity will cause wind erosion of roadbed structure, sand buried around roadbed and pavement, etc. The accumulation of blown sand will also have many impacts on the highway, such as damage to the road and an increase of economic costs, damage to the guardrail, and an impact on the anti-skid performance of asphalt pavement [3–5]. For the safe operation of highway in

the desert, many scholars have carried out a large number of studies on highway wind-sand damage by means of field observation [6], wind tunnel experiment [7,8], numerical simulation [9,10], and other means. Xie [11] studied the wind speed variation and the range where grits deposit easily on Liuyuan-Golmud Expressway when a sandy air current flows through field observation and wind tunnel test. Based on CFD numerical simulation, Li [12] described the aeolian sand transport process of sand rising, suspension, diffusion, deposition, and space-time concentration in the early entrainment stage. On the basis of these achievements, Shi [13] analyzed the process of grit transport and sediment when sandy air current flows through the subgrade section through the method of numerical simulation. In the underwater environment, sand movement is closely related to seabed shear stress threshold [14]. The studies on sandy air current mentioned above are mainly limited to the highway on flat terrain while the actual environment around desert highways is complex, with intricate dunes on both sides and variable wind direction. At present, there are few studies on the formation mechanism of highway sand damage in drifting sand dunes areas and in different terrain environments.

The wind field on the leeward slope of the dune is extremely complex and is one of the main factors affecting the movement of sediment. Walker [15] pointed out that the backflow zone of wind field on the leeward slope of the dune is the main influencing factor of dune formation, and there are mixed layers and strong turbulent erosion zones on the leeward side of the dune [16,17]. At the same time, some scholars focused on the microscopic process of interaction between turbulence and grits, confirming that instantaneous turbulence plays an important role in wind-sand activity [18,19].

In view of this, taking the test section of Wuhai-Maqin Expressway at Tengger Desert hinterland as the study object, on the basis of the sand accumulation measured along the highway and the wind data, this paper studies the change of highway sand accumulation and the formation mechanism of highway sand hazard in the drifting dunes area, which is for purposes of providing references for the construction and improvement of highway sand prevention systems in drifting dunes areas and providing guidance for future similar projects.

2. Field Experiment

2.1. Wind Speed Monitoring

The test section of Wuhai-Maqin Expressway is located in the hinterland of Tengger Desert, along which the dune chains are intricately distributed and the terrain is obviously undulating so that abundant sand sources, strong wind environment, and variable wind direction make drifting dunes a great threat to the highway (Figure 1). Through the field investigation, it was found that the depth of highway sand accumulation was more than 40 cm in 6 months and its distribution area was wide.

In the field investigation, the observation point was set on the west side of the highway in the test section (Figure 2). The height of wind cups is 2 m; the range is 0–70 m/s (resolution 0.1 m/s), and the wind direction range is 0–359°. The data, including wind speed, wind direction, temperature, and rainfall, were collected every minute and the observation time was from January 2021 to December 2021. According to the existing research results [20,21], the sand-driving wind speed at 2 m height (U_t) in Tengger Desert is about 5 m/s. According to scholars, grits can reach equilibrium state within 2 min after starting [22,23]. Therefore, this paper adopts the average wind speed within 2 min as the essential parameter of wind-sand environment evaluation.

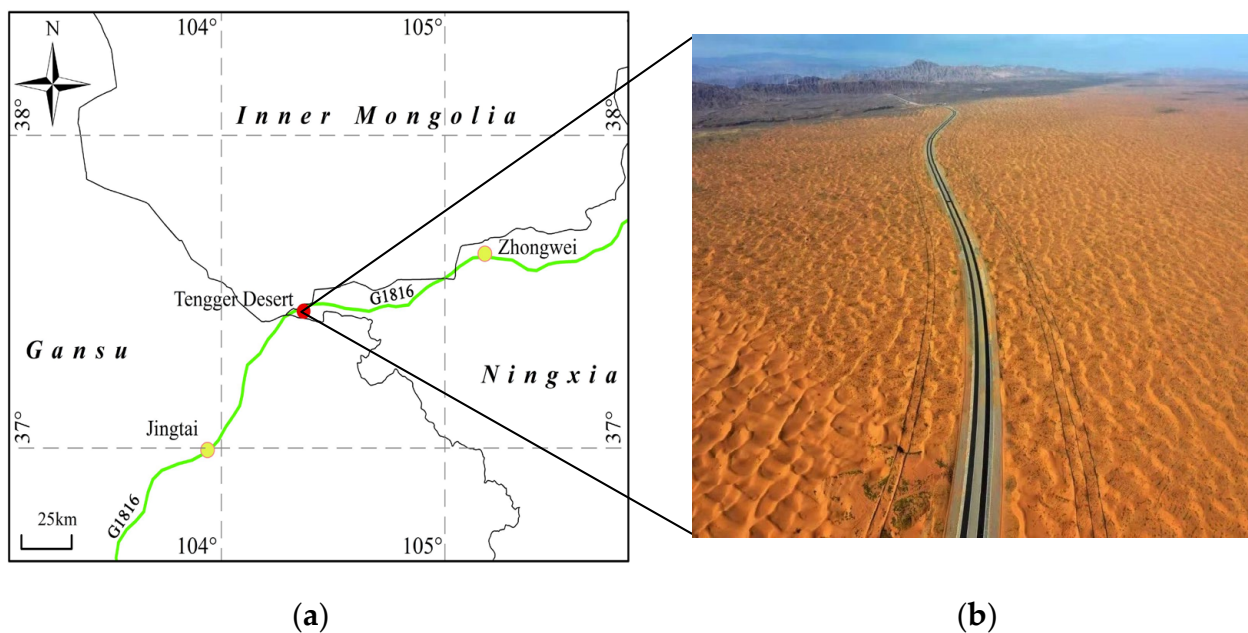


Figure 1. Picture of sand-accumulation environment in drifting sand dunes areas: (a) desert route and (b) aeolian landform environment.



Figure 2. Remote Weather Monitoring Station.

Assessment of non-directional wind speed change and wind speed probability distribution (b) are shown in Figure 3. As shown in Figure 3, in this region, the average annual wind speed (\bar{U}_2) in 2 min is 3.28 m/s and the average annual sand-rising wind speed is 7.18 m/s. The number of sand-rising days is more than 280 d, accounting for 77.3% of the total number of days in the whole year and the highest instantaneous wind speed is 18.6 m/s. Among them, strong winds with force greater than a strong breeze (wind

speed ≥ 10.8 m/s) lasted for 48 days, accounting for 14.1% of the total observed days. The frequency distribution of wind speed in this region is shown in Figure 3b, in which the frequency curve increases first and then decreases with the increase of wind speed, and the static wind frequency is 10.78% where the wind speed of 3–4 m/s reaches the peak value of the frequency curve, accounting for 16.5% of the total observed amount while the cumulative hours of sand-driving wind above 5 m/s were more than 1400 h, accounting for 17.8% of the total observed amount. Figure 3 indicates that the annual sand-driving wind is frequent and lasts for a long time, and the sand-wind activity is strong in this region.

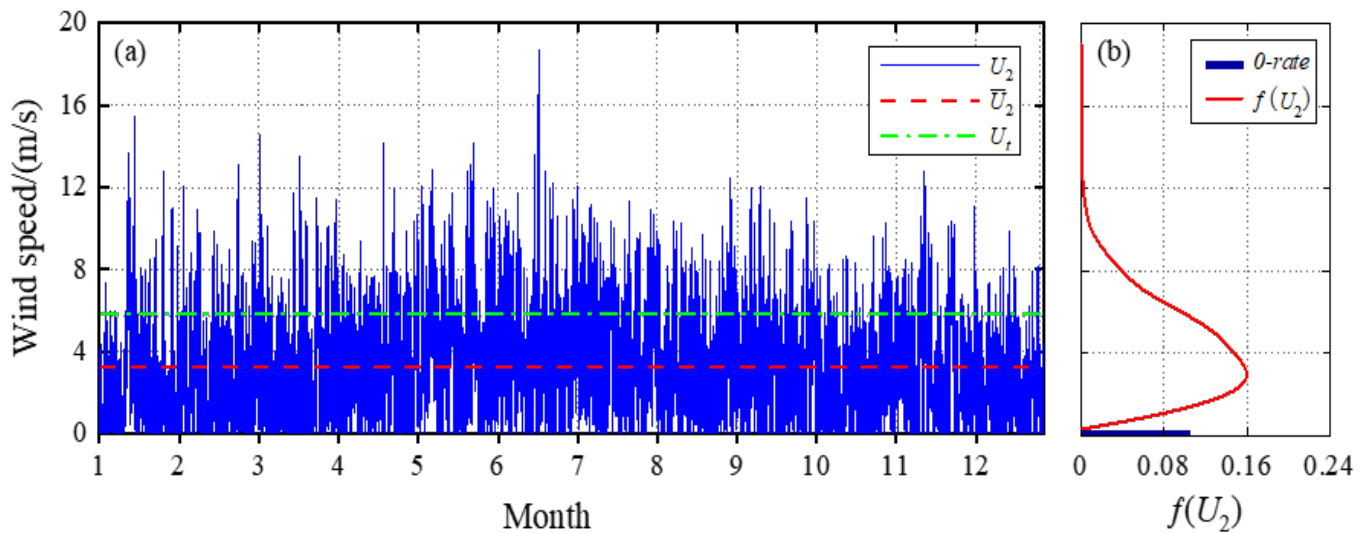


Figure 3. Distribution of non-directional wind speed variation (a) Distribution of non-directional wind speed variation (b) wind speed probability distribution (U_t represents the starting wind speed of sand particles at 2 m height in Tengger Desert; U_2 represents the 2 min annual observed variable wind speed in the region; \bar{U}_2 represents the 2 min average annual wind speed in the region).

2.2. Sand Transport Environment and Analysis

Drift Potential (DP) is widely used in the study of aeolian geomorphology or sand control engineering design and is the scale of surface wind energy of wind-sand activity [24,25]. According to the formula proposed by Fryberger [26], Drift Potential (DP), Resultant Drift Potential (RDP), and Resultant Drift Direction (RDD) can be calculated by the following equation:

$$DP = V^2(V - V_t)t \tag{1}$$

where DP represents drift potential of which the unit is VU; V_t represents the critical starting wind speed of sand particles at a height of 10 m, and V represents the wind speed not less than the critical starting speed of sand particles; both units are $\text{m}\cdot\text{s}^{-1}$. t represents the duration of sand-driving wind expressed by frequency in this paper. RDP (VU) and RDD ($^\circ$) are DP calculations based on vector synthesis laws; RDP is a vector synthesis of sand transport potential in 16 directions, reflecting net sand transport capacity. RDD represents the net trend of sand transport or the overall direction of aeolian sand transport under the influence of sand-raising wind in different directions. The directional wind variability index is the ratio of RDP to DP (RDP/DP), used to reflect the combination of regional wind direction and the complexity of wind signals [27].

It is of great importance to grasp the variation law of sand-drifting wind direction to explore the causes and control of sand damage [28]. The DP in different seasons in the study area is shown in Figure 4 and, under the influence of seasonal winds, the highway is easily buried from different directions by sand materials with the largest DP in spring (124.39 VU), followed by summer (108.97 VU) and winter (65.14 VU), and the smallest DP in autumn (64.89 VU). In the whole year, the largest Resultant Drift Potential (RDP) is 53.04 VU, which occurred in spring; the directional wind variability index is moderate ($RDP/DP = 0.43$); and

the sand drift direction is 125.92° so that sand materials are most easily transported from west to southeast. Following with spring, Resultant Drift Direction (*RDP*) is 53.04 VU in winter; the seasonal wind direction is single ($RDP/DP = 0.75$) and the sand drift direction is 64.41° so that sand materials are easily transported from west to northeast. Although the sand-driving wind has a long duration and strong dust concentration in summer, the seasonal wind direction is variable ($RDP/DP = 0.38$) and gale weather is frequent, accounting for the low *RDP* (41.65 VU), final sand transport direction 162.33° , and the fact that sand materials are easily transported from north to southeast. In autumn, with little wind and variable wind direction, *DP* and *RDP* are the smallest (41.65 VU) and sand drift direction is 5.73° so that sand materials are easily transport to the northeast. The sand transport environment in each season is in the direction of west to east. In spring, the sand drift direction and the road direction intersect almost vertically (89.08°), and the *DP* and the *RDP* are also the largest, indicating that the sand transport environment in spring is strong. As a consequence, timely attention should be paid to highway protection and sand cleaning.

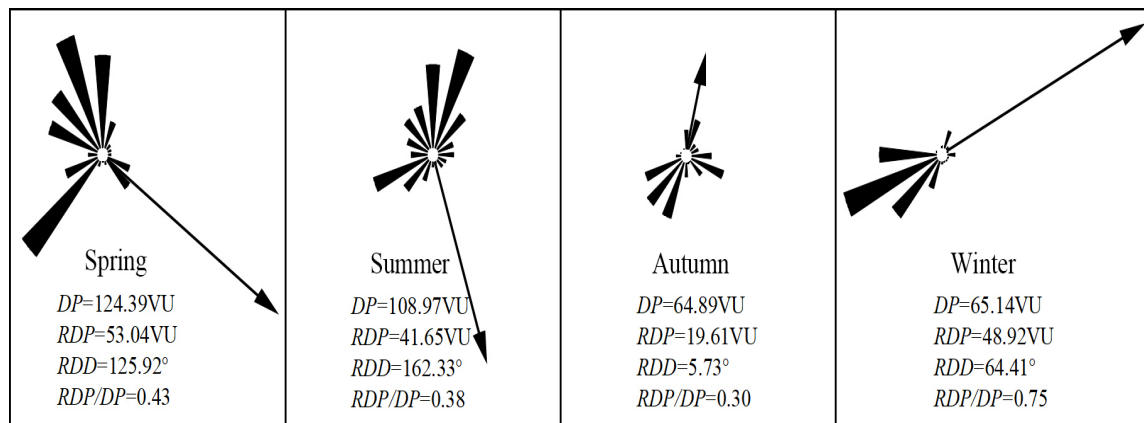


Figure 4. Sand drift potential of each season in the study area.

2.3. Sand Accumulation Observation and Analysis

The sand-accumulation data along the road were measured by UAV (unmanned aerial vehicle) oblique photography which has advantages of high efficiency, non-contact, and large range and can realize accurate measurement of dune movement and three-dimensional morphology [29,30]. The UAV was a DJI M300RTK multi-rotor UAV and the camera was Ruibo lens (Figure 5). Limited by experimental funds and site conditions, the observation time was from winter 2020 to summer 2021 and a total of three photography operations were conducted.



Figure 5. UAV for sand accumulation air survey and camera lens.

Highway surface sand deposition distribution was observed, during which the wind direction was dominated by southwest and the angle between the wind direction and observed path angle was not less than 50° ; as shown in Figure 6, the wind direction was from the top down. As time goes on, the dunes gradually move to the highway surface and accumulated sediment increases. In winter, road area sand is scattered covered on the road surface, the morphology of sand sedimentation is more dispersed and the thickness of sand accumulation on the highway surface is less than 2 cm. In spring and summer the morphology of sand accumulation is agminated forming sand burial and the maximum thickness of sand accumulation on the highway surface is more than 50 cm; specific road area sand sedimentation statistics are shown in Table 1. The main reason for the difference in sand-accumulation morphology in different seasons may be that the overall wind speed in winter in the study region is weak and the sandy air current is easy to saturate when it meets tall dunes, so that grits cannot cross the windward side of the dunes to form sediment, so only a small amount of the grit crossing the dunes disperses to the highway surface. In spring, the wind speed gradually increases and the sandy air current is not easy to saturate so as that the sand-carrying wind has a great push effect on the dune making the dune move slowly and form sand burial on the highway surface. After that, the wind is still strong in summer, and the dune continues to move along the dominant wind direction, resulting in the deterioration of sand burial.

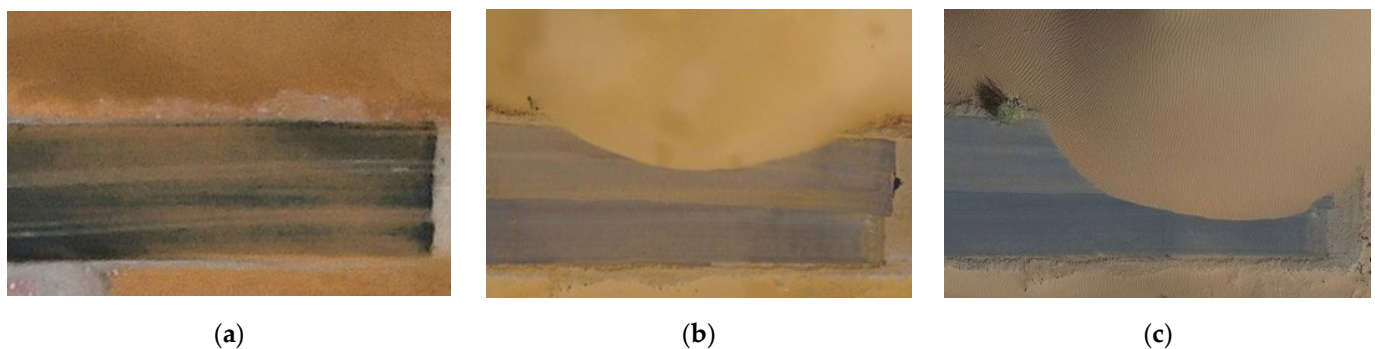


Figure 6. Change of sand-accumulation area on windward side of embankment: (a) winter in 2020, (b) spring in 2021, and (c) summer in 2021.

Table 1. Area of the sand sedimentation on highway surface statistical table.

Observation Time	Area of Sand Accumulation/m ²	Maximum Thickness/cm	Average Sand Accumulation Width/cm
2020-12	19	1.5	68
2021-04	24	21	70
2021-08	27	50	90

3. Numerical Simulation

3.1. Numerical Model

Due to the limited field observation data, the global wind conditions and sand sedimentation changes cannot be reflected. Numerical simulation is used to supplement the relevant test data. The overall size of the calculation domain model is $40\text{ m} \times 140\text{ m}$ and a distance of 40 m between the flow field entrance and the embankment section is reserved to ensure the full development of sandy air current in the flow field. According to the scale of the dune measured by UAV aerial photography, the half width of the dune model is 15 m with 3 m height and the embankment is 1 m high, of which the top surface is 14 m wide and the slope ratio is 1:3, the bottom width of the subgrade is 17 m, and the width of the asphalt pavement is 5 m. The embankment cross section models of windward and leeward dunes were established respectively, and their specific calculation size is shown in Figure 7.

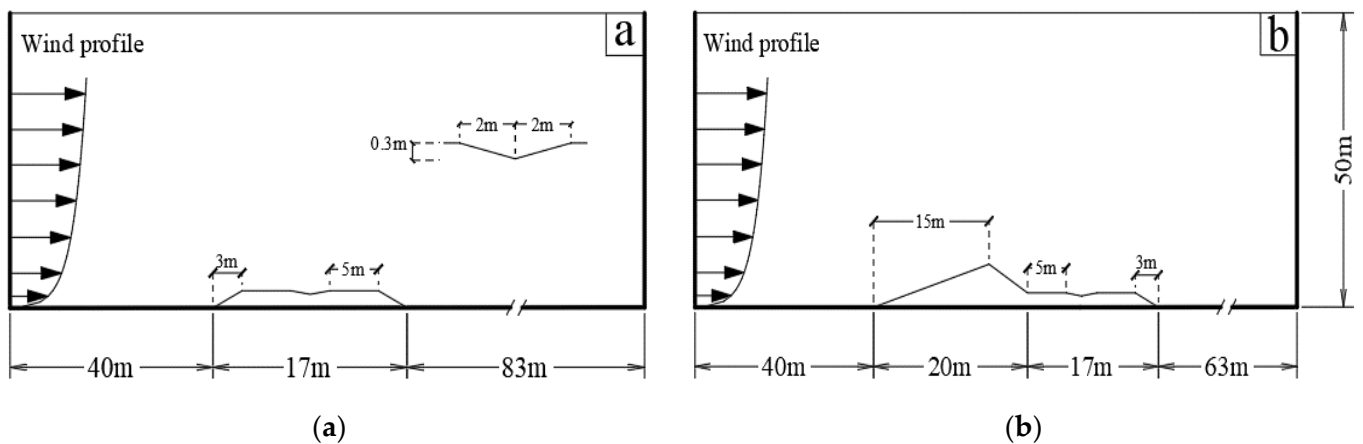


Figure 7. Flow field simulation domain—flat terrain (a) windward dune; (b) subgrade.

According to the field observation data, the annual sand-driving wind speed in this region is mainly concentrated in 5–18 m/s. In order to ensure the matching between the wind speed value in simulation and the engineering site, the prevailing wind of 8 m/s and the maximum wind speed of 18 m/s are selected for numerical simulation. The grit size in the study area is 0.075–0.25 mm. The grit size in the sandy air current is set as 100 μm ; grit density is 2650 kg/m^3 , and viscosity μ_s is 0.047 Pa·s [31]. The initial grit volume fraction is 3%; air density ρ_s is 1.225 kg/m^3 ; viscosity μ is 1.789×10^{-5} Pa·s; and inlet wind speed adopts a typical wind speed profile [32–34]. The equation of wind speed is as follows:

$$u(z) = \frac{u_*}{k} \ln \frac{z}{z_0} \quad (2)$$

where $u(z)$ is the velocity at the height z ; u_* is the friction of wind speed; K is von Karman coefficient set to 0.4; z is height; and z_0 is the roughness length.

Euler two-fluid model [35] supplemented with k - ϵ turbulent flow equation [35,36] was adopted as the calculation model and SIMPLEC was used as the solving algorithm. The wind speed in the study area is no more than 50 m/s and grits are mainly affected by gravity. The sandy air current can be regarded as incompressible fluid [37] and the heat exchange between sandy air current can be ignored; thus, the energy equation is not considered and the continuity equation, momentum equation, and k - ϵ turbulence model are considered in the study of wind-sand activity characteristics.

3.2. Verification of Numerical Simulation Results

In order to verify the reliability of the flow field in numerical simulation, this paper establishes a flow field model of the same size as the wind tunnel test in Reference [38]. In Reference [38], the wind tunnel test was used to study the law and characteristics of the wind-sand flow around the subgrade after the retaining wall was added, and the particle image velocimetry (PIV) was used to measure the particle velocity field on the leeward side, which was solved by CFD numerical simulation software. By analyzing the net wind speed around the windbreak wall, the horizontal velocity of sand particles and the deposition rate of sand particles on the track line, the influence of the setting position of the second windbreak wall on the sand accumulation effect of the railway is clarified, in order to provide reference data for the design of the later wind and sand prevention project. Based on the clear parameter settings, the horizontal wind speed changes at different heights under empty field conditions are simulated and compared with the wind speed profile of the wind tunnel test. The wind tunnel model established in Reference [38] has a size of 1.45 m \times 22 m, and the friction wind speed μ_* is 0.6395 m/s. The measured wind speed and the simulated wind speed in this paper are shown in Figure 8. It can be seen that the wind speed contour results of the wind tunnel test and numerical simulation are in good agreement. Therefore, the flow field structure and related calculation parameters set up in

this paper are reasonable and reliable, which can provide accurate calculation requirements for different subgrade models of Wuhai-Maqin Expressway.

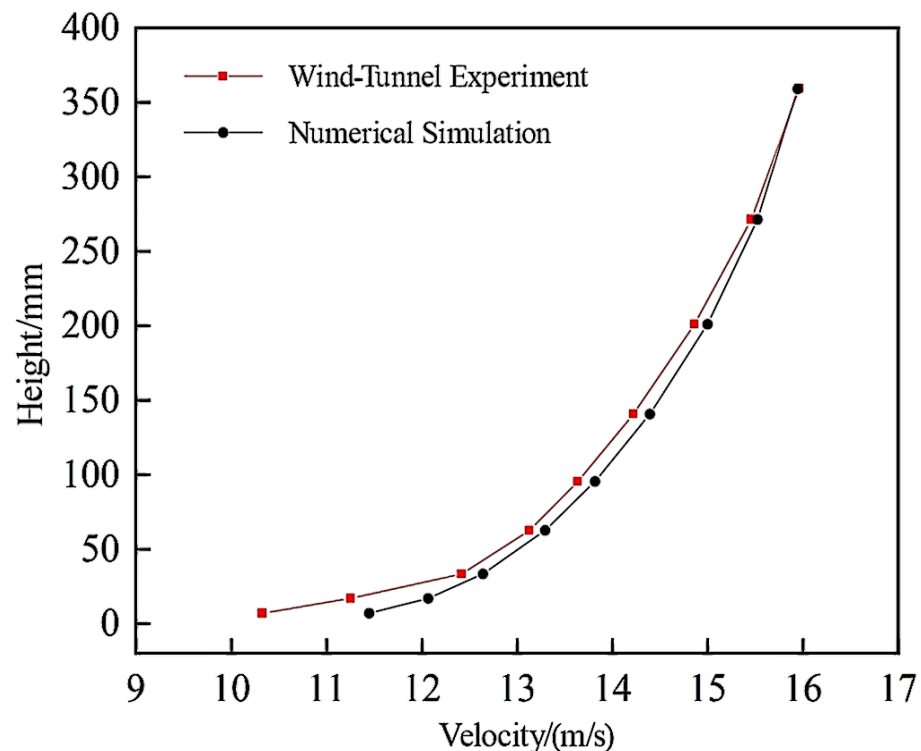


Figure 8. Comparison of wind speed profiles between wind tunnel test and numerical simulation.

3.3. Distribution Characteristics of Flow Field around Subgrade

Distribution characteristics of flow field around embankment when sand-carrying wind flows through flat terrain and where dunes exist are shown in Figure 9. It can be found that the change of terrain has a serious influence on the structure of the highway flow field. The sand-carrying air flows in from the leftmost entrance of the model. When wind flows to the windward slope foot of embankment or dune, the airflow deceleration zone appears at the windward slope foot due to the impediment of the sudden change of terrain and then the airflow rises along the slope with speed increasing gradually, leading to the formation of an airflow acceleration zone. When the airflow climbs to the top of the windward side embankment, the energy continuously gathers on the surface of the embankment, forming a high-speed zone. While on the leeward side of the dune, on account of the terrain declining sharply, the airflow velocity on the upper part of the highway surface is low, forming pressure difference in this area according to Bernoulli's principle, further resulting in vortex on the surface of the embankment. Then the air flow moves forward continuously and small fluctuations of wind speed occur at the depression in the center of the surface of the embankment. An airflow vortex is formed on account of the adverse pressure gradient generated by the impact of terrain when airflow passes through the leeward slope of the embankment. After that, the sandy air current crosses the cross section of the embankment, the energy changes gradually stabilize, and the original wind speed is restored. Finally, the sandy air current flows out of the air outlet on the right side of the model.

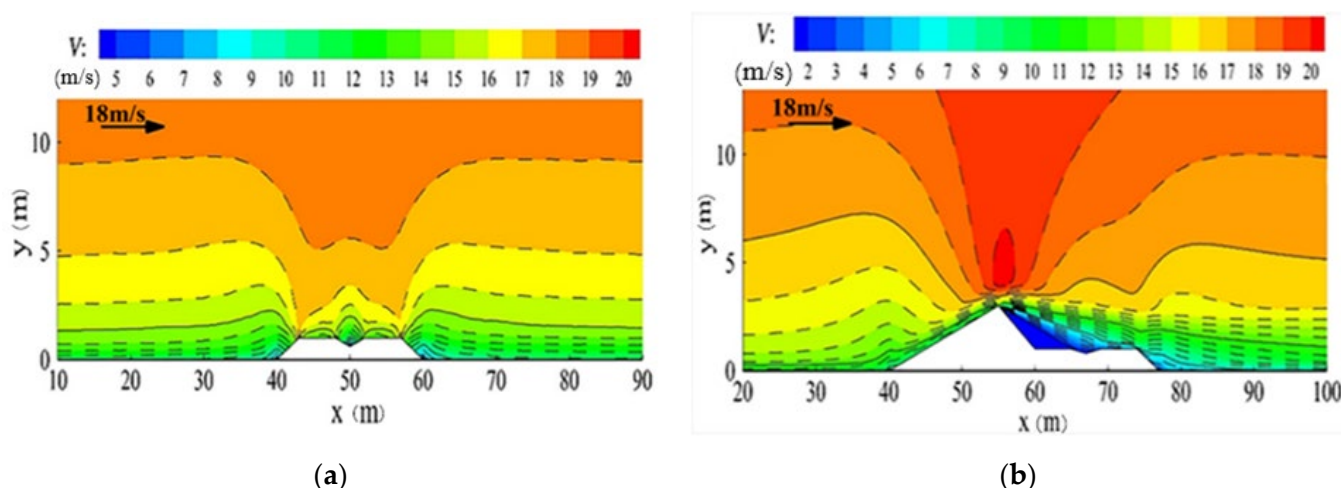


Figure 9. Distribution of wind-sand flow field around subgrade in flat terrain (a) and windward dune (b).

According to the variation characteristics of sandy air current in transit mentioned above, the grits pass slowly and tend to deposit in the deceleration zone, while in the acceleration zone, the grits tend to rise. At the high-speed zone, grits often pass quickly, while in the vortex region, the velocity of grits changes and can be sedimented or raised. When there are dunes around the embankment, the area of low-speed zone and vortex zone around the embankment both increase, providing more space for the sand-carrying wind to decelerate, in which case it is easy to cause the separation of grits and airflow.

3.4. Horizontal Wind Speed Changes at Different Heights

The changes of horizontal velocity of airflow on both sides of the embankment at the height of 0.3 m, 1.3 m, 3.3 m, and 3.3 m under different terrain conditions are shown in Figures 10 and 11 where the horizontal wind velocity at the height of 0.3 m and 1.3 m is within the influence range of dune and embankment height, thus the velocity curve is discontinuous. The horizontal wind velocity at the height of 3.3 m and 4 m presents an “M” shape distribution and if there is a dune, the maximum wind speed will concentrate on the top of the dune. When the wind speed is 18 m/s, the greatest reduction in wind speed is observed at the junction between the embankment and the dune where the wind speed at the foot of the leeward slope of the dune is 1.81 m/s at the height of 1.3 m, which is 87.9% lower than the original wind speed, followed by the leeward slope foot of embankment where the wind speed is 5.69 m/s and 4.78 m/s at the height of 0.3 m on flat terrain and dune, respectively, which are 55.7% and 62.8% lower than the original wind speed. The least reduction in wind speed is found at the windward side of the embankment and the dune where the wind speed at the height of 0.3 m is 8.52 m/s and 8.46 m/s, respectively, which are 33.6% and 34.1% lower than the original wind speed.

By comparing the horizontal wind speeds at different heights of the two kinds of flow fields—there are dunes or no dunes—around the embankment in Figures 9 and 10, it can be found that the structure of sandy air current around the road is closely related to the cross-section form of the embankment and the surrounding environment. Under different wind speeds of the same highway structure, the variation laws of sandy air velocity around the embankment are basically the same, while the variation range of wind speed gradient is more severe when sand-carrying wind with high speed passes the embankment. For each point on the embankment section, the areas with large decreasing range of wind speed are respectively the junction of dune and embankment, the leeward slope foot of embankment, and the leeward slope foot of embankment.

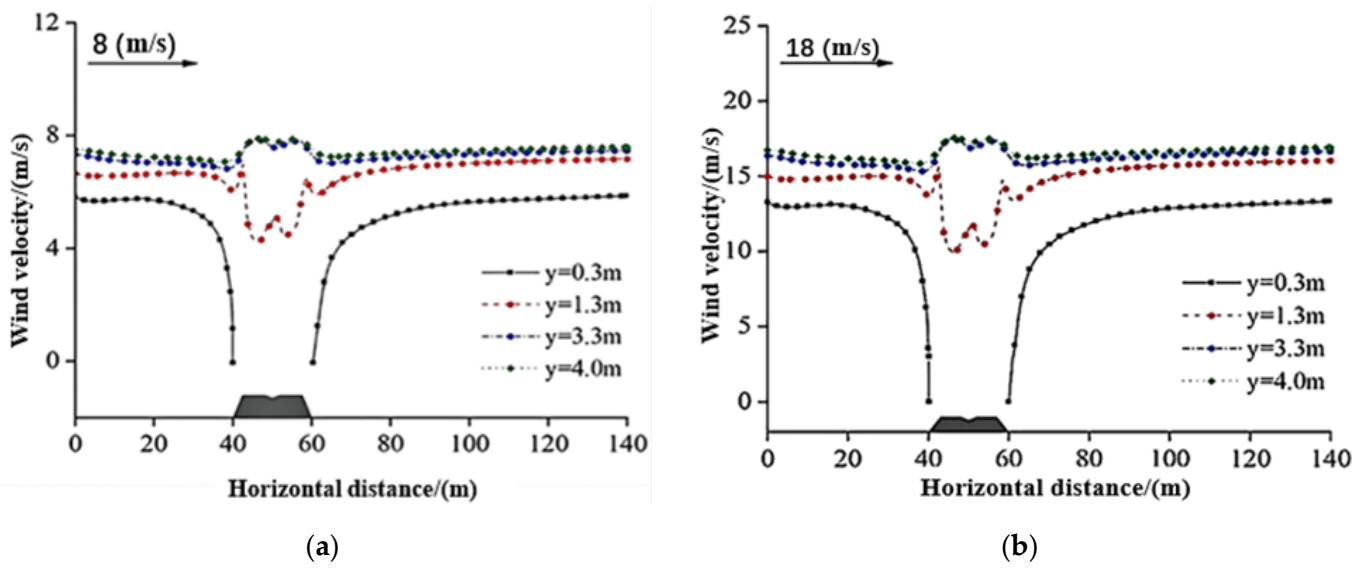


Figure 10. Horizontal wind speed at different heights from the surface of the embankment in flat terrain. (a) Wind speed of 8 m/s; (b) Wind speed of 18 m/s.

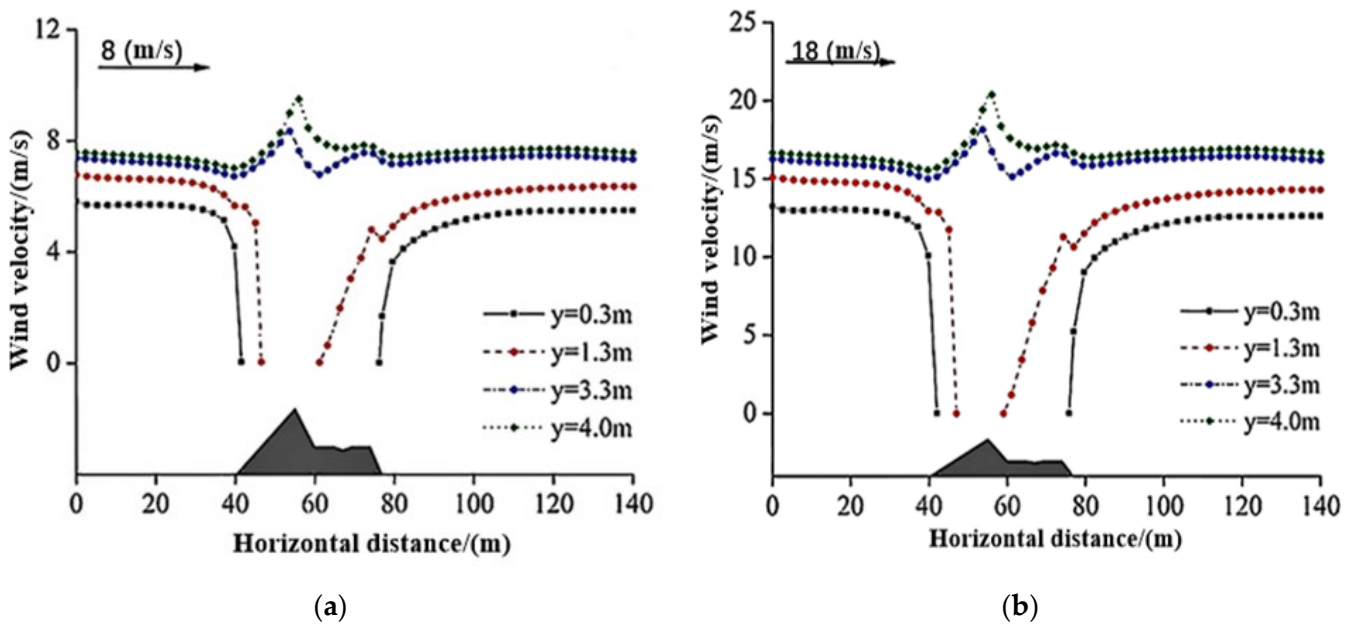


Figure 11. Horizontal wind speed at different heights from the surface of the windward dune embankment (a) Wind speed of 8 m/s; (b) Wind speed of 18 m/s.

3.5. Formation Mechanism of Sediment around Embankment

Given that there is a large quality difference between air flow and grits, when the running sandy air current encounters terrain obstruction or pressure difference, it will produce local resistance to reduce wind speed and also weaken the energy of airflow to transport grits, causing partial grits sediment. The distribution of grit size in flow field is shown in Figures 12 and 13; with the increase of wind speed, the sand accumulation at windward slope of the embankment and the dune gradually reduces, and the sand accumulation of leeward side has a tendency to increase. This is because, under the condition of high wind speed, although the velocity of sandy air current in obstacles side position is attenuated, wind velocity is still greater than the sand-driving wind velocity and sandy air current is unsaturated, so that the airflow has enough energy to drive most of the grits over obstacles. On the leeward side, after passing the low-speed area on the

surface of the embankment, the airflow enters the deceleration zone. The airflow energy decreases greatly, the sand easily forms a deposition, such that dunes develop on the windward side of the highway, and the distribution of sand accumulation on the surface of the embankment is uneven, accumulating sand dunes' leeward slope surface of the grits to the highway transport. However, under the condition of low wind speed, the sand-carrying airflow is saturated and when the wind speed is slightly attenuated, the airflow energy is not enough to drive the grits forward. Therefore, most of the grits will be sedimented in the deceleration zone on the windward side of the embankment. As shown in Figures 12 and 13, the sand-accumulation positions of the two flow field structures with low wind speed are mainly concentrated on the windward side. As can be seen in Figures 10 and 11, the airflow velocity changes significantly when the sandy air current passes through obstacles such as embankments and dunes. Under high wind speed conditions, sediment is easily formed in the position where the wind speed decreases greatly, while under low wind speed conditions, sediment is easily formed in the position where the wind speed first decreases.

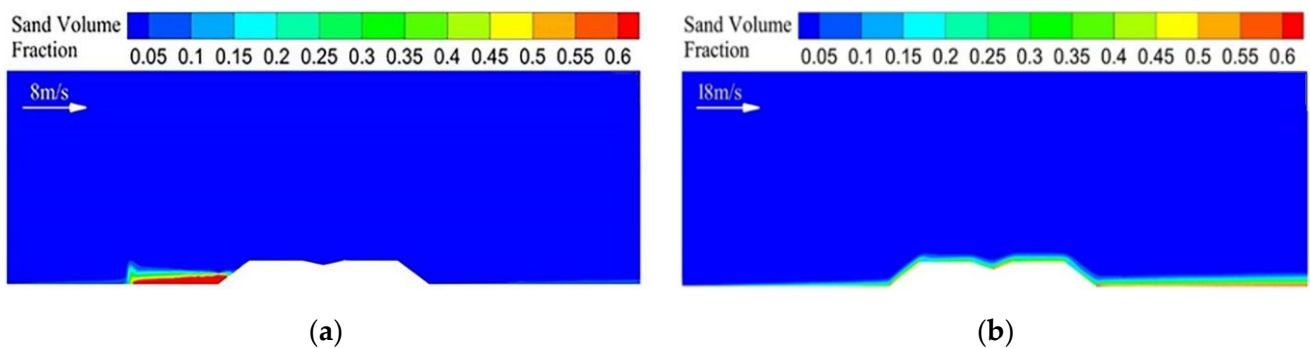


Figure 12. Distribution of sand volume fraction around embankment in flat terrain (a) Wind speed of 8 m/s; (b) Wind speed of 18 m/s.

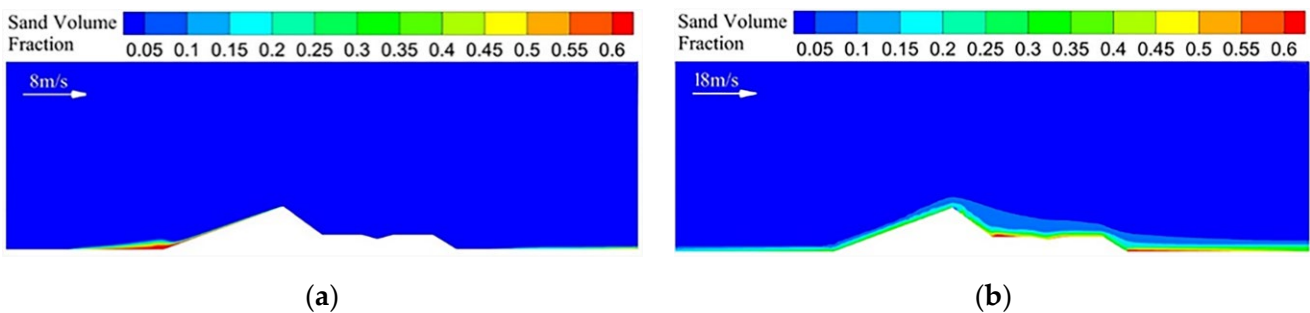


Figure 13. Distribution of sand volume fraction around embankment on the dune's windward side (a) Wind speed of 8 m/s; (b) Wind speed of 18 m/s.

4. Discussion

Through the statistical experiment of the sediment in the test section, the sand burial situation of subgrade with different terrain sections was observed. During the observation period, the angle between the dominant sand-driving wind direction and the highway in the test section varied from 50° to 80° . Measuring the thickness of sediment reveals that when there are no sand dunes existing, sand sedimentation is mainly distributed at the slope foot on both sides of the highway and the windward side sedimented more grits than the leeward side, whereas less sediment accumulated on the surface of the highway (Figure 14a). The thickness of embankment windward sand burial is more than 4 cm; the thickness of leeward sand burial is more than 3 cm; and the thickness of the concave side in the middle of the highway sand burial is 4.1 cm. When the sand dune exists along the road, the sediment on the highway surface is obvious and the thickness of sand accumulation is negatively correlated with the distance from the dune (Figure 15b), in which the sand

burial at the junction of the slope and the dune is more than 55 cm and sand sedimentation thickness measured in the middle of the road surface is 19.5 cm. It can be summarized that when the distribution of dunes is along the road, it can affect the thickness and shape of sand accumulation on the highway surface.

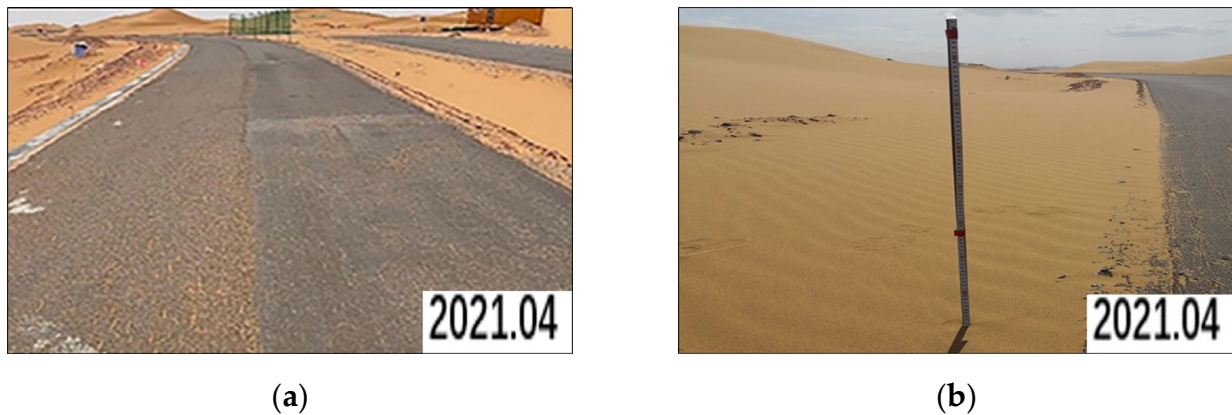


Figure 14. Sand accumulation of the highway in flat terrain (a) distribution of sediment (b) vertical measurement.

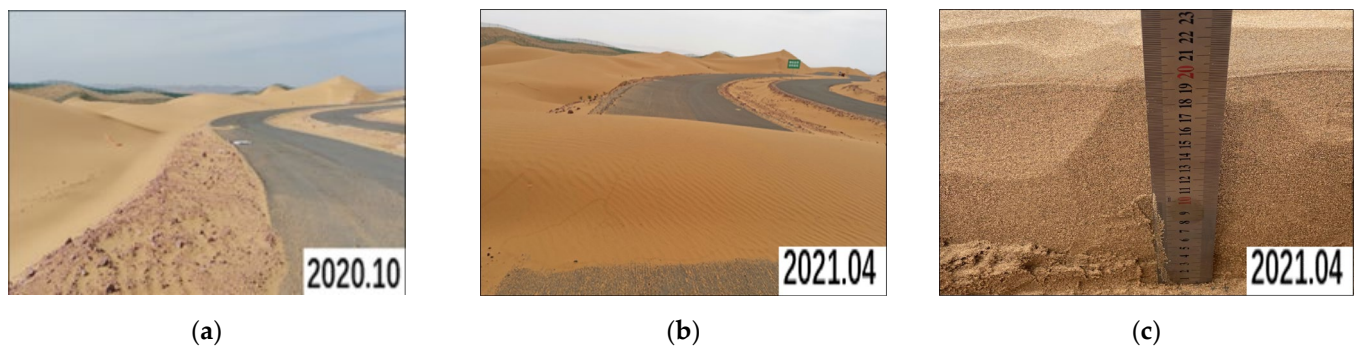


Figure 15. Sand accumulation of the highway on the dune's windward side (a) sediment distribution in October 2020 (b) sediment distribution in April 2021 (c) scale measurement.

The results of numerical simulation are consistent with those of the field investigation, which verifies the rationality of numerical simulation. The existence of the dunes interferes with the flow field around the embankment structure increases the probability of sand-accumulation sandy air current caused on the highway surface. On the other hand, the dunes themselves are not only obstacles for the sandy air current but also a source of highway sand accumulation. In addition, the grits carried by the sandy air current and the grits curled up on the windward side of the dune can be sand accumulation on the highway surface, and the dunes themselves also move in the direction of the prevailing wind, forming secondary sand sources to bury the highway over time.

5. Conclusions

On the basis of the field measured data and CFD numerical simulation, this paper studied the structure of the wind-sand flow field and the distribution law of sand accumulation around highways in different terrain environments in the drifting dune area under different wind speeds, and mainly drew the following conclusions:

- (1) Long-term wind action can make dunes move along the dominant wind direction, forming sand burial on the highway, thus affecting the normal operation of the highway.
- (2) The existence of dunes would affect the flow field structure and sand-accumulation position around the embankment. The airflow velocity gathers to the maximum at

the top of the dune. The airflow velocity changes in different wind speeds of the same highway structure are basically consistent.

- (3) For each point on the subgrade section, the airflow velocity at the junction of dune and subgrade decreases the most and it is easy to form sand accumulation. However, under the condition of low wind speed, dunes hinder the sand-carrying wind, and the airflow velocity decreases below the sand-driving wind on the windward slope of the dune, resulting in the deposition of most sand grains.
- (4) For the highway in the drifting dune area, the wind energy environment change trend should be studied in detail, sand protection should be set on the dominant wind direction side to control the dune movement speed, and the sand-accumulation situation on the highway should be checked regularly to clear the sand accumulation in time.

In practical engineering, highway sand accumulation is affected by wind direction, quicksand intensity, and construction technology. This study mainly focused on the formation mechanism of sand accumulation of subgrade in the initial state under ideal conditions of single wind direction and constant wind speed. However, in practice, highway sand accumulation is affected by a variety of factors. Our research results and conclusions provide a preliminary reference for practical engineering.

In this paper, the observation time of meteorological data for the analysis of wind-sand activity along the line was short, so that the sand transport potential in the observation area was similar to the calculation results of previous scholars; however, there is a gap. If a long-term wind-sand monitoring system can be established to increase the time span of wind-sand monitoring data, the characteristics of the wind-sand environment can be evaluated more accurately. For different desert road structure types, the degree of damage caused by wind-sand disaster is also different. The same road structure is used in field experimental observation and wind-sand flow simulation. In order to more accurately analyze and discuss the vulnerability of desert roads, it is appropriate to consider a variety of road structure forms in subsequent research. Our research methods and results can be extended to the construction of desert highways and the construction of sand prevention systems for roads in mobile dune areas to reduce sand hazard.

Author Contributions: Conceptualization, F.H. and Z.L.; methodology, F.H. and Z.L.; software, C.W. and Z.L.; validation, W.Y.; formal analysis, F.H. and L.L.; investigation, L.L.; resources, L.L. and W.Y.; data curation, C.W. and Z.L.; writing—original draft preparation, Z.L. and C.W.; writing-review and editing, C.W. and Z.L.; supervision, F.H. and L.L.; project administration, F.H.; funding acquisition, F.H. and W.Y. All authors have read and agreed to the published version of the manuscript.

Funding: This work was supported by the National Natural Science Foundation of China (grant numbers 51568037) and the Science and Technology Project of Ningxia Transportation Department (grant number 20200173).

Institutional Review Board Statement: This study did not involve humans or animals.

Informed Consent Statement: This study did not involve humans.

Data Availability Statement: This study did not report any data.

Conflicts of Interest: The authors declare no conflict of interest.

References

1. Zhang, K.C.; Qu, J.J.; Yu, Y.P.; Han, Q.; Wang, T.; An, Z.; Hu, F. Progress of Research on Wind-blown Sand Prevention and Control of Railways in China. *Adv. Earth Sci.* **2019**, *34*, 573–583.
2. Raffaele, L.; Bruno, L. Windblown sand action on civil structures: Definition and probabilistic modelling. *Eng. Struct.* **2019**, *178*, 88–101. [[CrossRef](#)]
3. Wang, C.; Li, S.; Li, Z.; Lei, J.; Chen, J. Effects of windblown sand damage on desert highway guardrails. *Nat. Hazards* **2020**, *103*, 283–298. [[CrossRef](#)]
4. Miri, A.; Middleton, N. Long-term impacts of dust storms on transport systems in south-eastern Iran. *Nat. Hazards* **2022**, *114*, 291–312. [[CrossRef](#)]

5. Pan, J.; Zhao, H.; Wang, Y.; Liu, G. The influence of aeolian sand on the anti-skid characteristics of asphalt pavement. *Materials* **2021**, *14*, 5523. [[CrossRef](#)] [[PubMed](#)]
6. Hu, G.; Dong, Z.; Zhang, Z.; Yang, L.; Hao, L.; Hesp, P.; Miot Da Silva, G. Wind regime and aeolian landforms on the eastern shore of Qinghai Lake, Northeastern Tibetan Plateau, China. *J. Arid Environ.* **2021**, *188*, 104451. [[CrossRef](#)]
7. Huang, N.; Gong, K.; Xu, B.; Zhao, J.; Dun, H.; He, W.; Xin, G. Investigations into the law of sand particle accumulation over railway subgrade with wind-break wall. *Eur. Phys. J. E* **2019**, *42*, 145. [[CrossRef](#)]
8. Li, S.; Li, C.; Yao, D.; Ge, X.; Zhang, G. Wind tunnel experiments for dynamic modeling and analysis of motion trajectories of wind-blown sands. *Eur. Phys. J. E* **2020**, *43*, 22. [[CrossRef](#)]
9. He, W.; Huang, N.; Xu, B.; Wang, W. Numerical simulation of wind-sand movement in the reversed flow region of a sand dune with a bridge built downstream. *Eur. Phys. J. E* **2018**, *41*, 53. [[CrossRef](#)]
10. Xin, G.; Huang, N.; Zhang, J.; Dun, H. Investigations into the design of sand control fence for Gobi buildings. *Aeolian Res.* **2021**, *49*, 100662. [[CrossRef](#)]
11. Xie, S.; Qu, J.; Zhang, K.; Han, Q.; Pang, Y. The mechanism of sand damage at the Fushaliang section of the Liuyuan-Golmud expressway. *Aeolian Res.* **2021**, *48*, 100648. [[CrossRef](#)]
12. Yintang, L.; Yi, G. Numerical simulation of aeolian dusty sand transport in a marginal desert region at the early entrainment stage. *Geomorphology* **2008**, *100*, 335–344.
13. Shi, L.; Jiang, F.; Han, F. Numerical simulation of response law of wind-blown sand flow around the railway embankment. *Tiedao Xuebao/J. China Railw. Soc.* **2014**, *36*, 82–87.
14. Leone, E.; Kobayashi, N.; Francone, A.; Bartolo, S.D.; Strafella, D.; D’Alessandro, F.; Tomasicchio, G.R. Use of Nanosilica for Increasing Dune Erosion Resistance during a Sea Storm. *J. Mar. Sci. Eng.* **2021**, *9*, 620. [[CrossRef](#)]
15. Walker, I.J. Secondary airflow and sediment transport in the lee of a reversing dune. *Earth Surf. Proc. Land.* **1999**, *24*, 437–448. [[CrossRef](#)]
16. Yin, Y.; Ding, W. A novel cloud model prediction for surface roughness based on multidimensional & multi-rules reasoning. *Jixie Gongcheng Xuebao/J. Mech. Eng.* **2016**, *52*, 204–212.
17. Wang, W.; Huang, N.; Dun, H. Analysis of wind-sand movement over sand dune with different railway forms downstream. *Lixue Xuebao/Chin. J. Theor. Appl. Mech.* **2020**, *52*, 680–688.
18. Schönfeldt, H.-J.; Löwis, S.v. Turbulence-driven saltation in the atmospheric surface layer. *Meteorol. Z.* **2003**, *12*, 257–268. [[CrossRef](#)]
19. Wiggs, G.F.S.; Weaver, C.M. Turbulent flow structures and aeolian sediment transport over a barchan sand dune. *Geophys. Res. Lett.* **2012**, *39*, 1–7. [[CrossRef](#)]
20. Zhang, K.; Qu, J.; An, Z. Characteristics of wind-blown sand and near-surface wind regime in the Tengger Desert, China. *Aeolian Res.* **2012**, *6*, 83–88. [[CrossRef](#)]
21. Zhang, K.C.; An, Z.S.; He, M.Z. Aeolian sand environments and disaster prevention along Zhongwei section of the Wuhai-Maqin Highway. *Arid Land Geogr.* **2021**, *44*, 983–991.
22. Zhang, Z.S.; Dong, Z.B.; Zhao, A.G. Effect of different time intervals in assessing sand drift potential. *Arid Land Geogr.* **2010**, *33*, 177–182.
23. Pearce, K.I.; Walker, I.J. Frequency and magnitude biases in the ‘Fryberger’ model, with implications for characterizing geomorphically effective winds. *Geomorphology* **2005**, *68*, 39–55. [[CrossRef](#)]
24. Xue, L.; Li, C.; Zheng, Z.; Shen, W.; Wang, H. Classification of Stability of Surrounding Rock Based on Two-Dimensional Cloud and Apriori. *Tiedao Xuebao/J. China Railw. Soc.* **2020**, *42*, 121–128.
25. Yizhaq, H.; Xu, Z.; Ashkenazy, Y. The effect of wind speed averaging time on the calculation of sand drift potential: New scaling laws. *Earth Planet. Sci. Lett.* **2020**, *544*, 116373. [[CrossRef](#)]
26. Fryberger, S.G. *Dune Forms and Wind Regime*; United States Government Printing Office: Washington, DC, USA, 1979; pp. 137–169.
27. Luo, F.; Gao, J.; Xin, Z.; Bian, K.; Hao, Y.; Liu, F. Characteristics of sand-driving wind regime and sediment transport in northeast edge of Ulan Buh Desert. *Nongye Gongcheng Xuebao/Trans. Chin. Soc. Agric. Eng.* **2019**, *35*, 145–152.
28. Cheng, J.; Jiang, F.; Xue, C.; Xin, G.; Li, K.; Yang, Y. Characteristics of the disastrous wind-sand environment along railways in the Gobi area of Xinjiang, China. *Atmos. Environ.* **2015**, *102*, 344–354. [[CrossRef](#)]
29. Li, J.; Wang, J.; Wang, R.; Guo, J.; Luo, X.; Li, Y.; Cui, W. Monitoring of moving speed of dunes along the Yellow River based on UAV technology and analysis of influencing factors. *J. Agric. Eng.* **2021**, *37*, 57–64.
30. Nolet, C.; van Puijenbroek, M.; Suomalainen, J.; Limpens, J.; Riksen, M. UAV-imaging to model growth response of marram grass to sand burial: Implications for coastal dune development. *Aeolian Res.* **2018**, *31*, 50–61. [[CrossRef](#)]
31. Cheng, J.; Xin, G.; Zhi, L.; Jiang, F. Unloading Characteristics of Sand-drift in Wind-shallow Areas along Railway and the Effect of Sand Removal by Force of Wind. *Sci. Rep. UK* **2017**, *7*, 41462. [[CrossRef](#)]
32. Tennekes, H. The logarithmic wind profile. *J. Atmos. Sci.* **1973**, *30*, 234–238. [[CrossRef](#)]
33. Bauer, B.O.; Houser, C.A.; Nickling, W.G. Analysis of velocity profile measurements from wind-tunnel experiments with saltation. *Geomorphology* **2004**, *59*, 81–98. [[CrossRef](#)]
34. Feng, S.; Ning, H. Computational simulations of blown sand fluxes over the surfaces of complex microtopography. *Environ. Modell. Softw.* **2010**, *25*, 362–367. [[CrossRef](#)]

35. Cheng, J.; Zhi, L.; Xue, C.; Jiang, F. Control Law of Lower Air Deflector for Sand Flow Field along Railway. *Zhongguo Tiedao Kexue/China Railw. Sci.* **2017**, *38*, 16–23.
36. Xin, G.; Cheng, J.; Yang, Y. Study on effect of characteristics of hanging-type concrete sand barrier opening and wind-sand field along railway. *Tiedao Xuebao/J. China Railw. Soc.* **2016**, *38*, 99–107.
37. Chen, B.; Cheng, J.; Xin, L.; Wang, R. Effectiveness of hole plate-type sand barriers in reducing aeolian sediment flux: Evaluation of effect of hole size. *Aeolian Res.* **2019**, *38*, 1–12. [[CrossRef](#)]
38. Xin, G.; Huang, N.; Zhang, J. Wind tunnel experiment on sand accumulation mechanism and optimization measures of windbreak wall along railway in windy area. *J. Mech.* **2020**, *52*, 635–644.